Published in final edited form as:
J Immunol. 2011 November 15; 187(10): 4987–4997. doi:10.4049/jimmunol.1102173.

On the Plasticity of Regulatory T Cell Function

Meenu R. Pillai[1], **Lauren W. Collison**[1,6], **Xiaohua Wang**[1,7], **David Finkelstein**[2], **Jerold E. Rehg**[3], **Kelli Boyd**[3,8], **Andrea L. Szymczak-Workman**[1], **Teresa Doggett**[5], **Thomas S. Griffith**[4], **Thomas A. Ferguson**[5], and **Dario A. A. Vignali**[1,*]

[1]Department of Immunology, St. Jude Children's Research Hospital, Memphis, TN 38105, USA

[2]Bioinformatics, St. Jude Children's Research Hospital, Memphis, TN 38105, USA

[3]Department of Pathology, St. Jude Children's Research Hospital, Memphis, TN 38105, USA

[4]Department of Urology, University of Iowa, Iowa city, IW 52242, USA

[5]Department of Ophthalmology and Visual Sciences, Washington University School of Medicine, St. Louis, MO 63110, USA

Abstract

Regulatory T cells (T_{regs}) can suppress a wide variety of cell types, in diverse organ sites and inflammatory conditions. While T_{regs} possess multiple suppressive mechanisms, the number required for maximal function is unclear. Furthermore, whether any inter-relationship or cross-regulatory mechanisms exist to orchestrate and control their utilization is unknown. Here we assessed the functional capacity of T_{regs} lacking the ability to secrete both interleukin-10 (IL-10) and interleukin-35 (IL-35), which individually are required for maximal T_{reg} activity. Surprisingly, IL-10/IL-35-double deficient T_{regs} were fully functional *in vitro* and *in vivo*. Loss of IL-10 and IL-35 was compensated for by a concurrent increase in cathepsin E (*Ctse*) expression, enhanced TRAIL (*Tnfsf10*) expression and soluble TRAIL release, rendering IL-10/IL-35-double deficient T_{regs} functionally dependent on TRAIL *in vitro* and *in vivo*. Lastly, while C57BL/6 T_{regs} are normally IL-10/IL-35-dependent, BALB/c T_{regs}, which express high levels of CTSE and enhanced TRAIL expression, are TRAIL-dependent by default. These data reveal that cross-regulatory pathways exist that control the utilization of suppressive mechanisms, thereby providing T_{reg} functional plasticity.

INTRODUCTION

Regulatory T cells (T_{regs}) play a key role in maintaining immune tolerance, preventing autoimmune diseases and limiting inflammatory conditions (1–3). A unique and important feature of T_{regs} is the brevity and flexibility of their regulatory capacity. T_{regs} can suppress an array of different cells types [including $CD4^+$ T cells [Th1/Th2/Th17] (4), $CD8^+$ T cells (5), B cells (4, 6), dendritic cells (7) and osteoclasts (8)] in a variety of inflammatory conditions and in distinct tissue locations. The ability of T_{regs} to suppress a broad range of targets in a variety of scenarios can be attributed to the numerous mechanisms employed by T_{regs} to mediate their function (2, 9). However, it is not clear whether all these mechanisms are equally important or if they have non-redundant roles under different inflammatory settings. Indeed, it was recently reported that T_{regs} may have specialized mechanisms for

*Correspondence: vignali.lab@stjude.org.
[6]Present address: Opexa Therapeutics, The Woodlands, TX 77381, USA.
[7]Present address: Albert Einstein College of Medicine, Bronx, NY 10461, USA.
[8]Present address: Department of Pathology, Microbiology and Immunology, Vanderbilt University Medical Center, Nashville, TN. 37232, USA.

controlling specific cell types, as T_{regs} appear to require IRF-4, T-bet and STAT3 to suppress Th2, Th1 and Th17 cells, respectively (10–12). However, it is unclear which T_{reg} mechanisms are used under specific conditions, how many mechanisms are required for maximal T_{reg} function and whether there is any crosstalk between the various regulatory mechanisms utilized. While it is well established that Foxp3 is a key transcription factor critical for the stability of T_{regs} (13), whether there is stability or plasticity in the regulatory mechanisms used by T_{regs} is unclear.

T_{regs} utilize multiple mechanisms to mediate their function, with the immunosuppressive cytokines TGF-β, IL-10 and IL-35 contributing significantly (14–16). IL-10 is important for T_{reg} function *in vitro* and *in vivo*, especially in the gut (17, 18). IL-35 is a recently discovered heterodimeric cytokine composed of *Ebi3* (also part of IL-27) and *Il12a/p35* (also part of IL-12) that is uniquely expressed by T_{regs}, but not by T_{conv} cells, and is required for maximal T_{reg} function (16). While the loss of either IL-10 or IL-35 significantly reduces T_{reg} function, they do not become completely dysfunctional and deficient mice do not exhibit the lethal multiorgan inflammatory disease seen in Scurfy or *Foxp3*$^{-/-}$ mice that lack T_{regs} (19, 20). Thus, in the present study we speculated that T_{regs} that lacked both IL-10 and IL-35 might exhibit a more profound functional defect and that this approach could be used to assess the relative contributions of different suppressive mechanisms. Alternatively, given the importance of T_{regs} in the maintenance of immune homeostasis, as yet unknown compensatory mechanisms may be triggered that attempt to restore immune balance. These possibilities were tested in this study.

MATERIALS AND METHODS

Mice

Ebi3$^{-/-}$ mice (C57BL/6: now 100% C57BL/6 by microsatellite analysis performed by Charles River) were provided by R. Blumberg and T. Kuo, *Il10*$^{-/-}$ mice were provided by T. Geiger, *Tnfsf10*$^{-/-}$ mice were provided by D. Green, and *Foxp3*$^{-/-}$ were provided by J. Ihle with permission from A. Rudensky. TGFβRII.DN, *Il12a*$^{-/-}$, *Rag1*$^{-/-}$, C57BL/6, BALB/c and B6.PL mice were purchased from the Jackson Laboratory. All animal experiments were performed in American Association for the Accreditation of Laboratory Animal Care-accredited, *Helicobacter*-free, MNV-free, specific-pathogen-free facilities in the St. Jude Animal Resource Center following national, state and institutional guidelines. Animal protocols were approved by the St Jude Animal Care and Use Committee. Spleens and lymph nodes from *Tnfrsf10b*$^{-/-}$ (DR5$^{-/-}$) mice were provided by T. Ferguson, with approval of the Washington University Animal Care and Use Committee.

Cell purification, staining and flow cytometric analysis

T_{conv} (CD4^{+}CD25^{-} CD45RB^{hi}) cells and T_{regs} (CD4^{+}CD25^{+}CD45RB^{lo}) from spleens and lymph nodes of either knockout or wild type C57BL/6 mice were positively sorted by FACS following staining with fluorochrome-conjugated antibodies: anti-mouse CD4, anti-mouse CD45RB and anti-mouse CD25 (Biolegend, San Diego, CA). The cells were sorted on a Reflection (i-Cyt, Champaign, IL) or on a MoFlo (Dako-Cytomation, Fort Collins, CO). For flow cytometric analysis, purified T_{regs} were cultured as described and stained with anti-TRAIL-PE antibody (eBioscience, San Diego, CA) at the indicated time points after culture in presence of rIL2 (1000IU/ml). CTSE intracellular staining was performed as previously described (21). Briefly, freshly isolated T_{regs} were fixed with formaldehyde and permeabilized with Triton X-100 for 2 min prior to staining with anti-CTSE antibody (R&D). Cells were analyzed on a FACS Calibur (Beckman Coulter, Brea, CA) and data analyzed using FlowJo.

Messenger RNA isolation, cDNA synthesis and quantitative PCR

Purified T_{regs} from wild type C57BL/6 mice or knockout mice were activated in the presence of anti-CD3 and anti-CD28 coated beads or cultured in combination with T_{conv} cells at 4:1 (T_{conv}: T_{regs}) ratio for 48h. Where indicated for TRAIL expression, cells were activated in presence of IL2 (1000 IU/ml) and cells collected from RNA isolation at indicated time points. Cells were resorted based on their congenic markers where indicated. RNA was isolated using Qiagen micro or mini RNA kit following manufacturer's instructions. RNA was quantified using a nanodrop spectrophotometer, and equal amount of total RNA in each sample was reverse-transcribed with the high capacity cDNA reverse-transcription kit (Applied Biosystems) following the manufacturer's guidelines. TaqMan primers and probes were designed with Primer Express software and were synthesized by the St Jude Hartwell Center for Biotechnology and Bioinformatics. The primers for CTSE were CTSE forward, CAACCTCTGGGTCCCTTC, CTSE reverse, TGATTCCCTACCTCCGTG, CTSE probe, CATGCAAGGCACACCCAG. TRAIL-R2 (DR5) forward primer, TGCTGCTCAAGTGGCGC, DR5 Reverse primer, GGCATCCAGCAGATGGTTG, Trail forward primer, CCTCTCGGAAAGGGCATTC, TRAIL reverse primer, TCCTGCTCGATGACCAGCT Actin forward, ACCCACACTGTGCCCATCTAC, Actin Reverse, AGCCAAGTCCAGACGCAGG and Actin probe, AGGGCTATGCTCTCCCTCACGCCA. Equal volume of cDNA samples were used in a qPCR reaction with primer probes and amplified for 40 cycles using an ABI prism 7900 Sequence Detection System instrument according to the manufacturer's protocol. Relative quantification of mRNA expression was carried out using the comparative CT (critical threshold) method as described in the ABI User Bulletin number 2 (http://docs.appliedbiosystems.com/pebiodocs/04303859.pdf). Here the amount of target mRNA is normalized to the endogenous beta-actin expression and is calculated by the formula $2^{\Delta\Delta CT}$.

Immunoprecipitation and western blotting

Immunoprecipitation and immunoblotting for CTSE were performed as previously described (21). T_{conv}, wild type or knockout T_{reg} were purified from spleens as described. Equal numbers of nT_{regs} and T_{conv} cells were lysed with lysis buffer. To all supernatants, lysis buffer containing 0.1% Tween 20, 50 mM HEPES, 150 mM NaCl, 1 mM EDTA, 2.5 mM EGTA, and 1 complete protease inhibitor tablet (Roche, Indianapolis, IN) per 50 ml lysis buffer, was added. Supernatants were immunoprecipitated with anti-mouse CTSE (R&D systems) and Protein G-sepharose beads. Immunoprecipitates were resolved by 10 % SDS-PAGE (Invitrogen Life Technologies), and blots were probed with a anti-goat HRP secondary antibody (Amersham Biosciences). Blots were developed using ECL (Amersham Biosciences) and autoradiography.

Preparation of anti-CD3/CD28-coated latex beads

4μM sulfate latex beads (Molecular Probes) were incubated overnight at room temperature with rotation in a 1:4 dilution of anti-CD3 and anti-CD28 antibody mix (13.3 μg/ml anti-CD3 (murine clone # 145-2c11, and 26.6 μg/ml anti-CD28 murine clone # 37.51, eBioscience). Beads were washed 3 times with 5mM phosphate buffer pH 6.5 and resuspended at 5×10^7/ml in sterile phosphate buffer with 2mM BSA.

In vitro T_{reg} suppression assay and Transwell™ T_{reg} assay

In vitro T_{reg} suppression assays were performed as described previously (16, 17, 22). Anti-CD3 and anti-CD28 coated beads used for T cell stimulation in these assays were prepared as described previously (17, 22). Briefly, T_{conv} and T_{reg} cells from wild type C57BL/6, *Ebi3*$^{-/-}$, *Il10*$^{-/-}$, *Ebi3*$^{-/-}$*Il10*$^{-/-}$ and *Il12a*$^{-/-}$*Il10*$^{-/-}$ mice were purified by FACS. Purified

T_{regs} were titrated in to a 96-well round bottom plate starting at a 2:1 ratio (T_{conv}:T_{regs}) with 5×10^4 T_{conv} cells. The cells were stimulated with anti-CD3/anti-CD28-coated latex beads for 72h. Cultures were pulsed with 1 μCi of [^{3}H]-thymidine for the final 8h of the 72h assay and harvested with a Packard harvester. The counts per minute (cpm) were determined using a Packard Matrix 96 direct counter (Packard Biosciences).

In vitro Transwell™ suppression assays were performed as described previously to assess the ability of T_{regs} to suppress via soluble mediators (17, 22). T_{conv} and T_{reg} cells from wild type C57BL/6 mice, and T_{regs} from *Ebi3*$^{-/-}$, *Il10*$^{-/-}$, *Ebi3*$^{-/-}$ *Il10*$^{-/-}$ mice were purified by FACS. Wild type T_{conv} and wild type or knock out T_{reg} cells were cultured at a 2:1 ratio in the Transwell™ insert with a pore size of 0.4μM (Millipore, MA). Target wild type T_{conv} or *Tnfrsf10b*$^{-/-}$ (DR5$^{-/-}$) T_{conv} cells were activated in the bottom compartment of the Transwell™ plate with anti-CD3 and anti-CD28-coated latex beads for 72 h. Where indicated, neutralizing IL-10 mAb (JES5-2A5; BD Biosciences), neutralizing IL-35 mAb (V1.4C4.22), isotype control or DR5-Fc were added to standard T_{reg} assays and Transwell™ experiments at the concentrations indicated. Where indicated, T_{conv} cells were fixed at a 1:5 dilution of 20% formaldehyde in culture medium, incubated at room temperature for 20 min, and washed 3 to 5 times with medium prior to culture. After 64h in culture, top Transwell™ inserts were removed and [^{3}H]-thymidine was added directly to the responder T_{conv} in the bottom chambers of the Transwell™ plate for the final 8h of the 72h assay. Cultures were harvested with a Packard harvester. The cpm were determined using a Packard Matrix 96 direct counter (Packard Biosciences).

CTSE/TRAIL transfection assay

For *in vitro* assays with transfected 293T cells co cultured with T_{conv} cells, 293T cells were transfected with *Ctse* (murine CTSE in pIYneo [pCIneo (Clontech) with an IRES-YFP expression cassette]; provided by Dr. Paul Kayser) or *Tnfsf10* (murine TRAIL in pIGneo [pCIneo with IRES-GFP]; provided by Dr Thomas Griffith) alone or in combination. Post-transfection (48h), the cells were irradiated (3000 rads) and seeded at a density of 7×10^3 cells per well in the 96-well flat bottom plate. Purified C57BL/6 T_{conv} cells were added to the seeded plate at 8×10^4 per well and stimulated with anti-CD3 and anti-CD28 coated beads for 72 h with [^{3}H]-thymidine added during the last 8h of culture. T cell proliferation was calculated by subtracting the basal [^{3}H]-thymidine incorporation of irradiated 293T plus unstimulated T_{conv} cells.

T_{reg}-mediated control of homeostatic expansion

Homeostasis assays were performed as described previously (16, 23). Briefly, naïve Thy1.1$^+$ T_{conv} cells from B6.PL mice, which were used as “target” cells, and Thy1.2$^+$ wild type or knockout T_{regs} were purified by FACS. T_{conv} cells (2×10^6) and T_{regs} (5×10^5) were resuspended in 0.5 ml PBS plus 2% FBS and injected i.v. into *Rag1*$^{-/-}$ mice. Where indicated the mice were injected on day 0 and 3 with anti-TRAIL antibody (0.3mg) (provided by Thomas Griffith, University of Iowa) or isotype control antibody (0.3mg) (R&D systems). Mice were euthanized 7 days post transfer, and splenocytes were counted, stained and analyzed by flow cytometry using antibodies against CD4, Thy1.1, Thy1.2 (Biolegend) and Foxp3 (BD Biosciences). For each group, 6–8 mice were analyzed.

Inflammatory bowel disease model

A recovery model of colitis/IBD was used, with some modifications (14, 23). Briefly, *Rag1*$^{-/-}$ mice were injected i.v. with 0.5×10^6 of wild type or DR5$^{-/-}$ (CD4$^+$CD45RB^{hi}CD25$^-$) naïve T_{conv} cells to induce IBD. Mice were weighed at the time of injection (time 0) and every week on the same day. At the onset of clinical symptoms of colitis (approximately 4 weeks post T_{conv} cell transfer), the mice were divided into T_{reg}

recipient or no T_{reg} control groups. Purified T_{regs} from wild type, *Ebi3*$^{-/-}$, *Il10*$^{-/-}$ *or* *Ebi3*$^{-/-}$*Il10*$^{-/-}$ were injected i.p. All mice were weighed weekly and euthanized 32 days-post the initial T cell transfer. A recovery model of colitis/IBD was set up as described in the methods section. In experimental mice, the colons were collected, fixed in 10% neutral-buffered formalin 4 weeks after T_{reg} injection. The tissues were further processed, 4μm sections cut and stained with H&E. Pathology of the large intestine was scored in a blinded manner using a semi-quantitative scale as described previously (23). In summary, grade 0 was assigned when no changes were observed; grade 1, minimal inflammatory infiltrates present in the lamina propria with or without mild mucosal hyperplasia; grade 2, mild inflammation in the lamina propria with occasional extension into the submucosa, focal erosions, minimal to mild mucosal hyperplasia and minimal to moderate mucin depletion; grade 3, mild to moderate inflammation in the lamina propria and submucosa occasionally transmural with ulceration and moderate mucosal hyperplasia and mucin depletion; grade 4 marked inflammatory infiltrates commonly transmural with ulceration, marked mucosal hyperplasia and mucin depletion, and multifocal crypt necrosis; grade 5, marked transmural inflammation with ulceration, widespread crypt necrosis and loss of intestinal glands.

Foxp3$^{-/-}$ rescue model

The *Foxp3*$^{-/-}$ rescue model was performed as described previously (23). Briefly, wild type or knockout T_{regs} purified by FACS were injected (10^6) i.p. into 2–3 day old *Foxp3*$^{-/-}$ mice. Recovery from disease was monitored weekly and reported as a clinical score. Five macroscopic categories were utilized to generate a 6 point scoring system. Mice were scored on the first 4 categories based on whether they showed (score of 1) or did not show (score of 0) the following characteristics: (1) body size runted, (2) tail is scaly and/or with lesions, (3) ears small, scaly with or without lesions, and (4) eyelids scaly and/or not fully open. The final scoring parameter was monitoring the activity level of the mouse. A score of 0 was assigned if the mouse was normal. A score of 1 was assigned if the mouse's activity was moderately impaired, and a score of 2 assigned if the mouse was immobile. A combined score of 4 or greater was assigned moribund for longevity. Mice were euthanized 25 days post-transfer, spleen cells counted, stained and cell numbers determined by flow cytometry. Lung, liver and ear pinna were prepared for H&E analysis and the severity of inflammation was assessed and scored in a blinded manner by an experienced veterinary pathologist. The scoring system used for assessing inflammation was based on a simple algorithm for expressing inflammatory infiltrates in the lungs, liver and ear. The scores allotted to these three tissues were 0–9, 0–11 and 0–8, respectively, giving a maximum possible total of 28. Scoring criteria for each organ was as follows. The lung score was based upon inflammation in the peribronchiolar region, perivascular region, or interstitium. A score of 0–3 was assigned to each category with 0 being minimal or no inflammation, and scores of 1, 2, or 3 indicative of <10%, 10–50%, or >50%, respectively. The liver was scored based on 3 criteria. First, was the degree of portal tract inflammation with a score of 0 assigned to minimal or no inflammation. A score of 1, 2 or 3 was assigned if inflammation was associated with <25%, 25–75%, or >75% of the liver portal tracts, respectively. The second criteria related to portal/periseptal interface hepatitis. A focus of interface hepatitis associated with either a few or most of the portal tracts were scored 1 and 2, respectively. Two or more foci of interface hepatitis surrounding <50% or > 50% of the portal tracts or periseptae was scored 3 and 4 respectively. Third, foci of granulocytes and/or lymphocytes with or without necrotic hepatocytes that expand the sinusoid were considered foci of inflammation. The number of inflammatory foci in 10 contiguous 10X objective fields was counted and recorded as the average number of foci per 10X field and given a score of 0 to 4. A score of 0 was assigned when sinusoidal foci of inflammatory cells was absent. One focus or less per 10X field, two to four foci per 10X field, five to ten foci per 10X field and more than ten foci per 10X field was scored 1, 2, 3 and 4 respectively. The ear pinna was

similarly scored based on 2 parameters; the percent of the ear dermis with inflammatory infiltrates and the intensity of the dermal inflammation. For percent analysis, a score of 0 was assigned when the inflammatory cells in all segments were not beyond that of normal background level. A score of 1, 2, 3 or 4 was assigned when the average percent for the segments was <25%, 25–50%, 51–75% or >75%, respectively. The intensity of the inflammatory infiltrate in the dermis was assessed as being of a loose or dense nature. A score of 0 was assigned when inflammatory cells in the dermis was not beyond the normal background level. When all the inflammation was of the loose nature, a score of 1 was assigned. When there was a mixture of loose and dense inflammatory cell infiltrates a score of 2 was assigned when the loose form was dominant. A score of 3 was assigned when the dense form was dominant. A score of 4 was assigned when all of the inflammation was of a dense nature.

Affymetrix array and analysis

Wild type or knock out T_{regs} were purified by FACS and mRNA isolated using the Qiagen micro RNA kit (Qiagen). Quality was confirmed by UV spectrophotometry and by analysis on an Agilent 2100 Bioanalyzer (Agilent Technologies, Santa Clara, CA). Total RNA (100ng) was processed in the Hartwell Center for Biotechnology & Bioinformatics according to the Affymetrix eukaryote two-cycle target labeling protocol and arrayed on a Mouse-430v2 GeneChip array. The expression data from the Affymetrix U133 plus 2 arrays was analyzed as MAS 5.0 signal log-start transformed using the following formula: log signal = ln (signal +20). This transform improves data dispersion, normality and stabilizes the variance of the data (24). Statistical tests and batch effect removal was performed using Partek Genomics Suite (St Louis, MO). The $\log_2$ratio of *Ebi3*$^{-/-}$*Il10*$^{-/-}$ T_{reg} to wild type T_{reg} was calculated and the 20 most positively induced named genes were selected. The $\log_2$ ratios are calculated in STATA/SE 11.0 (College Station, TX) by the following formula: logratio A over B = log(exp(mean log signal A)/exp(mean log signal b))/log(2). Minimum selected gene had a log ratio of 1.65 which is 3.14 fold induced. Log ratios of the *Il10*$^{-/-}$ T_{reg} and the *Ebi3*$^{-/-}$ T_{reg} with respect to wild type were also defined and plotted with the logratio of *Ebi3*$^{-/-}$*Il10*$^{-/-}$ T_{reg} to wild type as a heat map using Spotfire Decision Site software (Figure 3A). T tests were then applied to each probeset to compare the *Ebi3*$^{-/-}$*Il10*$^{-/-}$ T_{reg} to wild type T_{reg} and single knock out T_{reg} samples and $\log_2$ratios were calculated. The p-value from the t tests were then $-\log_{10}$ transformed to create the significance score seen in the X-axis of the volcano plot Figure 3 B. A second series of t tests were performed to compare T_{reg} to T_{conv} and to develop a T_{reg} signature. Probe sets that had a p-value < 10^{-5}, an absolute value log ratio of T_{reg} versus T_{conv} of at least 3 ($\log_2$), and a defined gene name were selected for each category in the signature the mean was found. If a gene name appeared more than once then the mean data was averaged for that gene. The scores were calculated by finding the maximum and minimum values for each gene and then rescaling them from 0 to 1 by the following formula: $score_g$ = (observed $mean_g$ − minimum $mean_g$)/(maximum $mean_g$ − minimum $mean_g$) for each gene g. These gene scores were then sorted in descending order by the T_{reg}: T_{conv} log ratio that includes activated and resting cells and graphed as a Heat map in Spotfire Decision Site (not shown). The microarray data from this study has been submitted in to the GEO repository. Accession number: GSE29262. http://www.ncbi.nlm.nih.gov/geo/query/acc.cgi?acc=GSE29262.

Statistical analysis

Unless otherwise stated Students t test was used to determine statistical significance. All calculations were done using GraphPad software. A p-value less than 0.05 was considered significant.

RESULTS

T_{regs} that lack IL-10 and IL-35 maintain their suppressive activity

We first assessed the functional capacity of T_{regs} that lacked the ability to secrete IL-10 or IL-35 by generating *Ebi3*$^{-/-}$*Il10*$^{-/-}$ and *Il12a*$^{-/-}$*Il10*$^{-/-}$ mice (note that both *Ebi3* and *Il12a/p35* are required for IL-35 production) (16, 17). Purified wild type, *Ebi3*$^{-/-}$, *Il10*$^{-/-}$, *Ebi3*$^{-/-}$*Il10*$^{-/-}$ and *Il12a*$^{-/-}$*Il10*$^{-/-}$ T_{regs} were assessed in a standard T_{reg} assay [note that these double-deficient T_{regs} would not be able to secrete IL-10 or IL-35, and although *Ebi3* is also used by IL-27 and *Il12a/p35* is also used by IL-12, these cytokines are not produced by T_{regs} (16)]. Surprisingly, *Ebi3*$^{-/-}$*Il10*$^{-/-}$ and *Il12a*$^{-/-}$*Il10*$^{-/-}$ T_{reg} function was comparable or slightly better than wild type T_{regs} in suppressing their target conventional T cells (T_{conv}) cells (Figure 1A). We have previously shown that if T_{regs} are optimally stimulated by anti-CD3 and anti-CD28-coated beads and in contact with T_{conv} cells in the upper chamber (insert) of a Transwell™ plate, they can suppress third-party T_{conv} cells in the lower chamber across a semi-permeable membrane (17). Importantly, this suppression requires, and is limited to, IL-10 and IL-35. Thus, we anticipated that the loss of IL-10 and IL-35 would render *Ebi3*$^{-/-}$*Il10*$^{-/-}$ T_{regs} unable to suppress across a Transwell™. Strikingly, *Ebi3*$^{-/-}$*Il10*$^{-/-}$ T_{regs} suppressed T_{conv} cells across a Transwell™ comparable to their wild type counterparts, even though *Ebi3*$^{-/-}$ and *Il10*$^{-/-}$ T_{regs} were partially defective (Figure 1B). This equivalency in function was further supported by experiments with CFSE-labeled target T_{conv} cells and Transwell™ experiments with titrated *Ebi3*$^{-/-}$*Il10*$^{-/-}$ T_{regs} in presence of fixed or unfixed T_{conv} cells (Figure S1 A and B). These data suggests that *Ebi3*$^{-/-}$*Il10*$^{-/-}$ T_{regs}, unlike *Ebi3*$^{-/-}$ and the *Il10*$^{-/-}$ T_{regs} are functionally intact in *in vitro* suppression assays.

We next asked if *Ebi3*$^{-/-}$*Il10*$^{-/-}$ T_{regs} were functionally equivalent in several *in vivo* models. The adoptive transfer of T_{regs} into neonatal Scurfy or *Foxp3*$^{-/-}$ mice has been shown to restore normal immune homeostasis and prevent the lethal, systemic autoimmune disease that develops in these mice (19, 25, 26). Two day old neonatal *Foxp3*$^{-/-}$ mice were injected with 10^6 wild type, *Ebi3*$^{-/-}$, *Il10*$^{-/-}$ or *Ebi3*$^{-/-}$*Il10*$^{-/-}$ T_{regs}. Clinical symptoms, histological analysis and $CD4^+$ T cell numbers were determined when the mice were ~4 weeks old. Although no defects were observed with the *Ebi3*$^{-/-}$ T_{regs} recipients, increased histological scores were observed with *Il10*$^{-/-}$ T_{reg} recipients. In contrast, *Ebi3*$^{-/-}$*Il10*$^{-/-}$ T_{regs} were clearly capable of fully restoring immune homeostasis despite the loss of these two key regulatory cytokines (Figure S2 A–C). We also assessed the ability of these T_{reg} populations to rescue immune homeostasis in mixed bone marrow chimeras generated using a 50:50 mixture of bone marrow from *Foxp3*$^{-/-}$ mice and either wild type, *Ebi3*$^{-/-}$, *Il10*$^{-/-}$ or *Ebi3*$^{-/-}$*Il10*$^{-/-}$ mice transferred into *Rag1*$^{-/-}$ mice. Interestingly, significant defects were observed in the ability of *Ebi3*$^{-/-}$ and *Il10*$^{-/-}$ bone marrow to rescue the *Foxp3*$^{-/-}$ phenotype (Figure S2 D and E). In contrast, the *Foxp3*$^{-/-}$ bone marrow recipients of *Ebi3*$^{-/-}$*Il10*$^{-/-}$ T_{regs} were largely intact and comparable to their wild type T_{reg}, *Foxp3*$^{-/-}$ recipient counterparts (Figure S2 D and E).

T_{regs} have been shown to regulate the homeostatic expansion of T_{conv} cells in lymphopenic *Rag1*$^{-/-}$ mice (27–29). Purified wild type Thy1.1 T_{conv} cells, either alone or in presence of wild type, *Ebi3*$^{-/-}$, *Il10*$^{-/-}$, *Ebi3*$^{-/-}$*Il10*$^{-/-}$ or *Il12a*$^{-/-}$*Il10*$^{-/-}$ Thy1.2$^+$ T_{reg} cells, were adoptively transferred into *Rag1*$^{-/-}$ mice, and splenic Thy1.1 T_{conv} and Thy1.2 T_{reg} cell numbers (data not shown) determined seven days later. In the presence of wild type, but not *Ebi3*$^{-/-}$ or *Il10*$^{-/-}$ T_{regs}, T_{conv} cell expansion was significantly reduced (Figures 1C). Surprisingly, the capacity of *Ebi3*$^{-/-}$*Il10*$^{-/-}$ and *Il12a*$^{-/-}$*Il10*$^{-/-}$$T_{reg}$ cells to control T_{conv} cell expansion was comparable to wild type T_{regs}.

T_{regs} cure colitis in mice, a model for inflammatory bowel disease (IBD) in humans, in an IL-10- and IL-35-dependent manner (16, 30). Colitis in mice is induced experimentally by transferring low numbers of naïve $CD4^+CD45RB^{hi}CD25^-$ T_{conv} cells into *Rag1*$^{-/-}$ mice (31). Recovery from disease, marked by weight gain and decreased histopathology, is observed only in mice that receive purified T_{reg} cells approximately four weeks after the initial T_{conv} cell transfer (14). We used this recovery model of colitis to assess the functional capacity of *Ebi3*$^{-/-}$*Il10*$^{-/-}$ T_{regs} *in vivo*. Approximately 4 weeks post T_{conv} cell transfer, recipients developed clinical symptoms of colitis (monitored by weight loss) and were either left untreated or were treated with either wild type, *Ebi3*$^{-/-}$, *Il10*$^{-/-}$ or *Ebi3*$^{-/-}$*Il10*$^{-/-}$ T_{regs}. As expected, mice that did not receive T_{regs} continued to lose weight, and exhibited substantial histiocytic infiltration and goblet cell destruction during the subsequent four weeks (Figures 1D, 1E, and S2F). In contrast, the wild type T_{reg} recipients started to gain weight within a week of transfer. Despite previous studies clearly demonstrating the inability of *Ebi3*$^{-/-}$ or *Il10*$^{-/-}$ T_{regs} to cure colitis, weight gain and improved histological parameters were evident in the *Ebi3*$^{-/-}$*Il10*$^{-/-}$ T_{reg} recipients, suggesting that these double inhibitory cytokine-deficient T_{regs} had regained their regulatory potential (Figures 1D, 1E and S2F).

To rule out the possibility that this regulatory restoration had occurred as a consequence of their development in the absence of IL-10 and IL-35 and/or due to alternate cell-extrinsic mechanisms, we directly compared the suppressive capacity of wild type and *Ebi3*$^{-/-}$*Il10*$^{-/-}$ T_{regs} that had developed in the same environment. To address this possibility, we generated mixed bone marrow chimeras with a 1:1 ratio of congenically-marked $Thy1.1^+$ wild type bone marrow with $Thy\ 1.2^+$ wild type or *Ebi3*$^{-/-}$*Il10*$^{-/-}$ bone marrow into sublethally-irradiated *Rag1*$^{-/-}$ mice. Eight weeks post-transfer, T_{regs} were purified by FACS from the mixed bone marrow chimeras and assessed in *in vitro* Transwell™ and *in vivo* homeostasis assays. Chimera-derived *Ebi3*$^{-/-}$*Il10*$^{-/-}$ T_{regs} and wild type T_{regs} suppressed third party T_{conv} cells comparably across a Transwell™ (Figure 2A). In contrast, similarly prepared *Ebi3*$^{-/-}$ and *Il10*$^{-/-}$ T_{regs} were defective (data not shown). Furthermore, $Thy1.2^+$ *Ebi3*$^{-/-}$*Il10*$^{-/-}$ T_{regs} and wild type T_{regs} that had developed in the bone marrow chimeras suppressed T_{conv} expansion comparably in homeostasis assay (Figure 2B). Taken together, these data suggest that a cell-intrinsic modification had occurred in the *Ebi3*$^{-/-}$*Il10*$^{-/-}$ T_{regs} to render them functionally comparable to wild type T_{regs} in order to compensate for their inability to secrete IL-10 and IL-35.

Loss of IL-10/IL-35 results in a compensatory increase in CTSE

Given that *Ebi3*$^{-/-}$*Il10*$^{-/-}$ T_{regs} can suppress T_{conv} cells across a Transwell™, they had clearly acquired a suppressive mechanism that operated via a soluble mediator. Beyond IL-10 and IL-35, transforming growth factor-β (TGFβ) is the only other known cytokine or soluble factor that would likely function across a Transwell™ that has been suggested to play a role in T_{reg} function [note that cAMP and adenosine are highly labile inhibitors that are only active in very close proximity] (2, 3, 9). We assessed any potential role for TGFβ by comparing the capacity of wild type and *Ebi3*$^{-/-}$*Il10*$^{-/-}$ T_{regs} to suppress across a Transwell™ using third party T_{conv} cells from CD4-dnTGFβRII transgenic mice that are resistant to TGFβ-mediated suppression (32). The data clearly show that the suppressive capacity of wild type and *Ebi3*$^{-/-}$*Il10*$^{-/-}$ T_{regs} was comparable when T_{conv} cells resistant to TGFβ-mediated suppression were used as target cells (Figure S1C). This suggested that the compensatory suppressive mechanism used by *Ebi3*$^{-/-}$*Il10*$^{-/-}$ T_{regs} was not TGFβ.

To identify this compensatory suppressive mechanism, we compared the gene expression profile of wild type, *Ebi3*$^{-/-}$, *Il10*$^{-/-}$ and *Ebi3*$^{-/-}$*Il10*$^{-/-}$ T_{regs} using Affymetrix GeneChip arrays. We first generated a list of highly differentially expressed wild type T_{reg} signature genes, by comparison of the array profile with wild type T_{conv}, to determine if there were

any notable global changes in gene expression in wild type versus *Ebi3*$^{-/-}$*Il10*$^{-/-}$ T_{regs}. Minimal variations were observed in the expression (up or down) of 47 highly modulated T_{reg} signature genes (Data not shown). Indeed, global analysis revealed very few differences between wild type and *Ebi3*$^{-/-}$*Il10*$^{-/-}$ T_{regs} (Figures 3A, 3B and Data not shown). The two notable exceptions were *Ap1S3* (adaptor-related protein complex 1, sigma 3 subunit) and *Ctse* (cathepsin E) (Figures 3A, 3B). AP1S3 is the sigma subunit of the adaptor protein-1 (AP1) complex that is a component of the clathrin-coated vesicles associated with the trans-Golgi network (TGN) that mediate vesicular formation and transport (33). The significance of its up-regulation in *Ebi3*$^{-/-}$*Il10*$^{-/-}$ T_{regs} is unknown and was not selected for further study here. CTSE is an intracellular aspartic protease of the endolysosomal pathway that has been primarily implicated as a component of the antigen processing machinery for the MHC class II pathway (34). Quantitative PCR, immunoprecipitation/western blot analysis and intracellular staining with purified T_{regs} confirmed that CTSE mRNA and protein are highly up-regulated in *Il10*$^{-/-}$ and *Ebi3*$^{-/-}$*Il10*$^{-/-}$ T_{regs} compared with wild type and *Ebi3*$^{-/-}$ T_{regs} (Figure 3C–E and S3 A–C).

Interestingly, CTSE has been implicated in the cleavage and/or processing of TRAIL (TNF-related apoptosis-inducing ligand; *Tnfsf10*; tumor necrosis factor (ligand) superfamily, member 10), and its release from the cell surface (35, 36). TRAIL is a suppressive molecule of the TNF superfamily that can function in its surface bound form or as a soluble trimer (37, 38). TRAIL can mediate apoptosis, programmed necrosis (necroptosis) or suppress proliferation (37, 39). Furthermore, activated $CD4^{+}Foxp3^{+}$ T_{regs} and $CD8^{+}$ T_{regs} may express and utilize TRAIL as a suppressive mechanism (40, 41). Thus, we speculated that increased CTSE in *Ebi3*$^{-/-}$*Il10*$^{-/-}$ T_{regs} might result in an increase in the functional capacity of surface TRAIL and/or an increase the release of soluble TRAIL. To directly examine this possibility, 293T cells were transfected with expression plasmids encoding *Ctse* and/or *Tnfsf10* and used to assess the ability of TRAIL to limit T cell proliferation. TRAIL transfectants limited T cell proliferation and this was further enhanced in the presence of CTSE (Figure 4). These data suggest that CTSE may play a role in enhancing the function of TRAIL by either increasing its activity via processing or increasing the generation of soluble TRAIL. This data also raised the possibility that *Ebi3*$^{-/-}$*Il10*$^{-/-}$ T_{regs} are dependent on TRAIL for their suppressive activity, while wild type T_{regs} are not.

IL-10/IL-35 deficient T_{regs} suppress via TRAIL

We first assessed whether there were any changes in the level or rate of TRAIL expression during activation of wild type, *Ebi3*$^{-/-}$, *Il10*$^{-/-}$ or *Ebi3*$^{-/-}$*Il10*$^{-/-}$ T_{regs}. Minimal alterations in *Tnfsf10* (TRAIL) mRNA expression was observed over time or between the four T_{reg} population (Figures S3D). While all T_{reg} populations exhibited increased TRAIL surface expression following activation, *Ebi3*$^{-/-}$*Il10*$^{-/-}$ T_{regs} expressed significantly higher levels of TRAIL after 16h but not 24h, post-activation (Figure 5A, B and S3E). This suggested that the kinetics of TRAIL expression is accelerated in *Ebi3*$^{-/-}$*Il10*$^{-/-}$ T_{regs}. Interestingly, while IL10 appeared to influence CTSE expression (Figure 3C and E and S3 A–C), IL-35 may influence other parameters that influence TRAIL expression as *Ebi3*$^{-/-}$ T_{regs} expressed slightly higher levels of TRAIL at 16h compared with wild type or *Il10*$^{-/-}$ T_{regs} (Figure S3E).

We then used various approaches to determine the extent to which this accelerated TRAIL expression meant that the *Ebi3*$^{-/-}$*Il10*$^{-/-}$ T_{regs} were dependent on TRAIL-mediated suppression. TRAIL mediates its suppression in part via caspase-mediated apoptosis (37). Thus we asked if *Ebi3*$^{-/-}$*Il10*$^{-/-}$ T_{regs} mediated suppression in a caspase-dependent fashion by performing a Transwell™ suppression assay in the presence of the general caspase inhibitor z-VAD-Fmk or a vehicle control (42). Although wild type T_{reg} suppression was unaffected by z-VAD-Fmk or its DMSO vehicle control, *Ebi3*$^{-/-}$*Il10*$^{-/-}$ T_{reg} mediated

suppression was blocked (Figure 5C). These data suggest that *Ebi3*$^{-/-}$*Il10*$^{-/-}$ T_{regs} suppress T_{conv} proliferation via a caspase dependent pathway.

TRAIL signaling in the mouse is mediated through DR5 (death receptor 5; *Tnfrsf10b*; tumor necrosis factor receptor superfamily, member 10b; also known as TRAIL-R2) (43). Therefore, we first asked if the *Ebi3*$^{-/-}$*Il10*$^{-/-}$ T_{regs} were able to suppress *Tnfrsf10b*$^{-/-}$ T_{conv} cells (hereafter referred to as DR5$^{-/-}$) in conventional and Transwell™ suppression assays. As previously shown, wild type and *Ebi3*$^{-/-}$*Il10*$^{-/-}$ T_{regs} suppressed wild type T_{conv} cells comparably (Figure 6A). Furthermore, wild type T_{regs} could effectively suppress DR5$^{-/-}$ T_{conv} cells. However, *Ebi3*$^{-/-}$*Il10*$^{-/-}$ T_{regs} were less effective at suppressing DR5$^{-/-}$ T_{conv} cells in a standard T_{reg} assay (Figure 6A) and completely failed to suppress across a Transwell™ (Figure 6B). Secondly, we assessed whether a DR5-Fc fusion protein or an anti-TRAIL blocking antibody were able to inhibit *Ebi3*$^{-/-}$*Il10*$^{-/-}$ T_{reg}–mediated suppression of wild type T_{conv} cells. While DR5-Fc had a minimal effect on the suppression mediated by wild type T_{regs} across a Transwell™, blocked suppression by *Ebi3*$^{-/-}$*Il10*$^{-/-}$ T_{regs} in a dose dependent manner (Figure 6C). Similarly, anti-TRAIL, but not an isotype control antibody, reduced the suppressive capacity of *Ebi3*$^{-/-}$*Il10*$^{-/-}$, but not wild type, T_{regs} [note that this TRAIL mAb is known to block activity weakly *in vitro* but very effectively *in vivo* (44)] (Figure S4A). These results suggest that *Ebi3*$^{-/-}$*Il10*$^{-/-}$ T_{regs} mediate suppression across a Transwell™ *in vitro* via soluble TRAIL.

We then assessed the contribution of TRAIL-mediated suppression by *Ebi3*$^{-/-}$*Il10*$^{-/-}$ T_{regs} *in vivo*. First, congenic Thy1.1^{+} wild type T_{conv} cells were either injected into *Rag*$^{-/-}$ mice alone or in the presence of Thy1.2^{+} wild type or *Ebi3*$^{-/-}$*Il10*$^{-/-}$ T_{regs}. Isotype control antibody or anti-TRAIL was injected on days 0 and 3, and homeostatic expansion of the Thy1.1^{+} T_{conv} cells determined 7 days later. T_{conv} cell expansion, wild type T_{reg}-mediated suppression, and T_{reg} numbers were unaffected by the anti-TRAIL treatment (Figure 6D and data not shown). In striking contrast, TRAIL inhibition blocked the ability of *Ebi3*$^{-/-}$*Il10*$^{-/-}$ T_{regs} to suppress T_{conv} cell expansion *in vivo*.

Second, we assessed the extent to which the *Ebi3*$^{-/-}$*Il10*$^{-/-}$ T_{regs} could cure colitis induced by DR5$^{-/-}$ T_{conv} cells. The development and severity of colitis induced by wild type or DR5$^{-/-}$ T_{conv} cells in *Rag*$^{-/-}$ mice were comparable (Figure 6E, 6F and S4B). At the onset of clinical symptoms (5% loss of body weight; ~4 weeks), mice were treated with wild type or *Ebi3*$^{-/-}$*Il10*$^{-/-}$ T_{regs}. Wild type T_{reg} recipients gained weight and recovered from the clinical symptoms of colitis regardless of whether the disease had been induced by wild type or DR5$^{-/-}$ T_{conv} cells (Figure 6E and 6F). In contrast, *Ebi3*$^{-/-}$*Il10*$^{-/-}$ T_{regs} could cure colitis caused by wild type but not DR5$^{-/-}$ T_{conv} cells. Histological analysis of the colon 4 weeks post-T_{reg} treatment confirmed that *Ebi3*$^{-/-}$*Il10*$^{-/-}$ T_{regs} were unable to reverse DR5$^{-/-}$ T_{conv} cell-induced colitis (Figure S4B).

Third, if TRAIL was essential for *Ebi3*$^{-/-}$*Il10*$^{-/-}$ T_{reg}-mediated suppression, then its genetic deletion should abrogate their regulatory capacity. Our data suggest that although wild type and *Ebi3*$^{-/-}$*Il10*$^{-/-}$ T_{reg} could effectively mediate suppression of T_{conv} cells across a Transwell™, *Ebi3*$^{-/-}$*Il10*$^{-/-}$*Tnfsf10*$^{-/-}$ T_{regs} could not inhibit T_{conv} target cell proliferation (Figure 6G). Taken together these data clearly demonstrate that *Ebi3*$^{-/-}$*Il10*$^{-/-}$ T_{regs} require TRAIL for maximal suppressive function, and that soluble TRAIL appears to be their only mechanism of suppression. In contrast, wild type T_{regs} exhibit minimal TRAIL-dependence and use IL-35 and IL-10 as their soluble mediators of suppression.

Differential utilization of suppressive mechanisms by genetically distinct T_{regs}

Loss of IL-10 and IL-35 production by T_{regs} led to increased CTSE expression and subsequent dependence on TRAIL-mediated suppression. We questioned the extent to which

unmanipulated examples of this T_{reg} functional plasticity might exist. Differential CTSE expression has been reported in different inbred mouse strains (21). In particular, C57BL/6 mice express low levels of CTSE, while expression in BALB/c and 129 mice is high. We first confirmed these observations by assessing *Ctse* expression by qPCR and intracellular staining (Figure 7A and 7B). The results clearly indicate that BALB/c T_{regs} express higher levels of CTSE, consistent with previous observations (21). Next we assessed the kinetics of TRAIL surface expression on BALB/c T_{regs} following activation. Interestingly, BALB/c T_{regs} expressed slightly higher levels of surface TRAIL than C57BL/6 T_{regs}, particularly at 16h post-activation (Figure 7C). Indeed, the pattern of CTSE and TRAIL expression exhibited by BALB/c T_{regs} was analogous to observations made with *Ebi3*$^{-/-}$*Il10*$^{-/-}$ T_{regs} (compare Figures 3C, 3D and 5A with Figures 7A, 7B and 7C), and was consistent with previous suggestions (45). We then examined the suppressive capacity of BALB/c and C57BL/6 T_{regs} in presence or absence of reagents that block IL-10, IL-35 or TRAIL. While anti-IL-10 and the isotype control antibody had little effect on the suppression mediated by either T_{reg} population in a Transwell™ assay, IL-35 neutralizing mAb blocked suppression mediated by C57BL/6, but not BALB/c, T_{regs} (Figure 7D). In contrast, DR5-Fc inhibited suppression mediated by BALB/c, but not C57BL/6, T_{regs}. Thus C57BL/6 T_{regs} seems to be more dependent on IL-35, while BALB/c T_{regs} are dependent on TRAIL-mediated suppression. This raises the possibility that genetic variations predispose T_{regs} to preferential modes of immunosuppression.

DISCUSSION

T_{regs} can function in diverse anatomical locations and in a wide variety of immunological and disease settings (46). Consequently, the large array of suppressive mechanisms that T_{regs} are reported to possess may help them maintain immune homeostasis under diverse scenarios. Indeed, T_{regs} may have specialized mechanisms for controlling specific cell types as T_{regs} appear to require IRF-4, T-bet and STAT3 to suppress Th2, Th1 and Th17 cells, respectively (10–12). However, this may have a greater influence on their migratory behavior than the mechanisms they use to mediate suppression. Importantly, the relative importance of specific mechanisms of T_{reg} function and whether T_{regs} possess mechanistic flexibility has not been elucidated. Previous studies have reported that deficiency of IL-10 or IL-35 alone results in defective T_{reg} function (16, 18). Thus our finding that T_{regs} lacking IL-35 and IL-10 are fully functional, instead relying on TRAIL-mediated suppression as a primary mechanism of action, was very surprising. This implies that T_{regs} can exhibit remarkable functional plasticity and possess control mechanisms to compensate for the loss of key regulatory tools.

There is a reciprocal relationship in the expression of IL-10 and CTSE (47). Our data clearly show that *Ebi3*$^{-/-}$*Il10*$^{-/-}$ T_{regs} are dependent on TRAIL for their regulatory function *in vitro* and *in vivo*. Furthermore, our studies suggest that increased expression of CTSE enhances the rate and extent of TRAIL surface expression and TRAIL function in mediating T cell suppression. It is possible that CTSE may ‘process’ full length TRAIL to enhance its ligand binding and/or may mediate the cleavage of cell surface TRAIL to generate a soluble version. Soluble TRAIL is thought to be either secreted into microvesicles (48) or cleaved from the cell surface (49). While the precise mechanism by which CTSE enhances TRAIL function requires further elucidation, consistent with our results, previous studies have shown that proteolytic cleavage of TRAIL from the cell surface can be mediated by CTSE (35, 36). Thus in *Ebi3*$^{-/-}$*Il10*$^{-/-}$ T_{regs}, CTSE up-regulation may play a role in the generation of soluble TRAIL. In contrast, expression of IL-10 by wild type T_{regs} may suppress CTSE expression and thus reduce the contribution of TRAIL-mediated killing. These data also support the capacity of activated T_{regs} to utilize TRAIL (40, 41), and further highlight the complex inter-regulatory pathways modulated by inhibitory cytokines. However, TRAIL is

clearly not utilized by *Il10*$^{-/-}$ T_{regs}, emphasizing that loss of IL-35 expression also contributes to the ability of *Ebi3*$^{-/-}$*Il10*$^{-/-}$ T_{regs} to mediate suppression via TRAIL. While the contribution of IL35 in minimizing TRAIL-mediated suppression remains to be defined, it is noteworthy that *Ebi3*$^{-/-}$ T_{regs} exhibit accelerated TRAIL expression following activation, raising the possibility that IL-35 may suppress a distinct component of the TRAIL processing machinery.

An important question is the extent of the physiological impact of the T_{reg} functional plasticity revealed in our study has applicability. As shown here and in previous studies, substantial differences in CTSE expression occur in different mouse strains with, BALB/c mice expressing high levels of CTSE while C57BL/6 mice expressing low levels (21, 45). Interestingly, BALB/c T_{regs} appeared to phenocopy *Ebi3*$^{-/-}$*Il10*$^{-/-}$ T_{regs} in terms of their pattern of CTSE and TRAIL expression and thus their dominant dependence on TRAIL-mediated suppression. Although there are certainly multiple genetic factors that might underlie differences in the function of T_{regs} from distinct genetic backgrounds, our data suggest differential CTSE expression may be one contributing factor. Whether this is related to the necessity of T_{regs} to adapt to the different T helper cell bias exhibited in different mouse strains remains to be determined (50, 51). Given that previous studies have shown that T_{regs} can utilize different transcription factors to tackle different Th environments (10–12), it is possible that these may underlie the differential utilization of T_{reg} suppressive mechanisms observed here. This remarkable T_{reg} functional plasticity may also be important in providing a backup mechanism in scenarios where IL-10 and IL-35 production and/or signaling may be perturbed and thus may empower T_{regs} with the ability to adjust to different environmental settings. Lastly, the possibility that TRAIL may be a legitimate target for the treatment of diseases impacted by excessive T_{reg} function, such as cancer, requires further study.

Supplementary Material

Refer to Web version on PubMed Central for supplementary material.

Abbreviations

CTSE	Cathepsin E
TRAIL	TNF-related apoptosis-inducing ligand
Tnfsf10	tumor necrosis factor (ligand) superfamily, member 10
DR5	death receptor 5
TRAIL-R2; Tnfrsf10b	tumor necrosis factor receptor superfamily, member 10b
IBD	inflammatory bowel disease

Acknowledgments

The authors would like to thank Doug Green and Benny Chain for advice, Rick Blumberg, Doug Green, Sasha Rudensky, Terry Geiger and Jim Ihle for mice, Amanda Burton and Kate Vignali for technical assistance, Creg Workman for help with Affymetrix analysis, Karen Forbes, Amy Krause and Ashley Castellaw for mouse colony maintenance and breeding, Richard Cross, Greig Lennon and Stephanie Morgan for FACS, the staff of the Shared Animal Resource Center at St. Jude for the animal husbandry, and the Hartwell Center for Biotechnology and Bioinformatics at St Jude for real-time PCR primer/probe synthesis.

This work was supported by the National Institutes of Health (R01 AI39480 and AI091977 to D.A.A.V.; R01 EY06765, EY015570 and P30 EY02687 to T.A.F.; R01 CA109446 to T.G.; F32 AI072816 to L.W.C.), Research to Prevent Blindness, New York (to T.A.F.), NCI Comprehensive Cancer Center Support CORE grant (CA21765, to D.A.A.V.), and the American Lebanese Syrian Associated Charities (ALSAC, to D.A.A.V.)

REFERENCES

1. Sakaguchi S, Sakaguchi N, Shimizu J, Yamazaki S, Sakihama T, Itoh M, Kuniyasu Y, Nomura T, Toda M, Takahashi T. Immunologic tolerance maintained by CD25+ CD4+ regulatory T cells: their common role in controlling autoimmunity, tumor immunity, and transplantation tolerance. Immunol Rev. 2001; 182:18–32. [PubMed: 11722621]
2. Vignali DA, Collison LW, Workman CJ. How regulatory T cells work. Nat Rev Immunol. 2008; 8:523–532. [PubMed: 18566595]
3. Tang Q, Bluestone JA. The Foxp3+ regulatory T cell: a jack of all trades, master of regulation. Nat Immunol. 2008; 9:239–244. [PubMed: 18285775]
4. Thornton AM, Shevach EM. CD4+CD25+ immunoregulatory T cells suppress polyclonal T cell activation in vitro by inhibiting interleukin 2 production. J Exp Med. 1998; 188:287–296. [PubMed: 9670041]
5. Park Y, Oh SJ, Chung DH. CD4(+)CD25(+) regulatory T cells attenuate Hypersensitivity Pneumonitis by suppressing IFN-gamma production by CD4(+) and CD8(+) T cells. J Leukoc Biol. 2009; 86:1427–1437. [PubMed: 19741155]
6. Yang ZZ, Novak AJ, Stenson MJ, Witzig TE, Ansell SM. Intratumoral CD4+CD25+ regulatory T-cell-mediated suppression of infiltrating CD4+ T cells in B-cell non-Hodgkin lymphoma. Blood. 2006; 107:3639–3646. [PubMed: 16403912]
7. Tadokoro CE, Shakhar G, Shen S, Ding Y, Lino AC, Maraver A, Lafaille JJ, Dustin ML. Regulatory T cells inhibit stable contacts between CD4+ T cells and dendritic cells in vivo. J Exp Med. 2006; 203:505–511. [PubMed: 16533880]
8. Zaiss MM, Axmann R, Zwerina J, Polzer K, Guckel E, Skapenko A, Schulze-Koops H, Horwood N, Cope A, Schett G. Treg cells suppress osteoclast formation: a new link between the immune system and bone. Arthritis Rheum. 2007; 56:4104–4112. [PubMed: 18050211]
9. Vignali D. How many mechanisms do regulatory T cells need? European Journal of Immunology. 2008; 38:908–911. [PubMed: 18395857]
10. Zheng Y, Chaudhry A, Kas A, deRoos P, Kim JM, Chu TT, Corcoran L, Treuting P, Klein U, Rudensky AY. Regulatory T-cell suppressor program co-opts transcription factor IRF4 to control T(H)2 responses. Nature. 2009; 458:351–356. [PubMed: 19182775]
11. Koch MA, Tucker-Heard G, Perdue NR, Killebrew JR, Urdahl KB, Campbell DJ. The transcription factor T-bet controls regulatory T cell homeostasis and function during type 1 inflammation. Nat Immunol. 2009; 10:595–602. [PubMed: 19412181]
12. Chaudhry A, Rudra D, Treuting P, Samstein RM, Liang Y, Kas A, Rudensky AY. CD4+ regulatory T cells control TH17 responses in a Stat3-dependent manner. Science. 2009; 326:986–991. [PubMed: 19797626]
13. Williams LM, Rudensky AY. Maintenance of the Foxp3-dependent developmental program in mature regulatory T cells requires continued expression of Foxp3. Nat Immunol. 2007; 8:277–284. [PubMed: 17220892]
14. Mottet C, Uhlig HH, Powrie F. Cutting edge: cure of colitis by CD4+CD25+ regulatory T cells. J Immunol. 2003; 170:3939–3943. [PubMed: 12682220]
15. Marie JC, Letterio JJ, Gavin M, Rudensky AY. TGF-beta1 maintains suppressor function and Foxp3 expression in CD4+CD25+ regulatory T cells. J Exp Med. 2005; 201:1061–1067. [PubMed: 15809351]
16. Collison LW, Workman CJ, Kuo TT, Boyd K, Wang Y, Vignali KM, Cross R, Sehy D, Blumberg RS, Vignali DA. The inhibitory cytokine IL-35 contributes to regulatory T-cell function. Nature. 2007; 450:566–569. [PubMed: 18033300]
17. Collison LW, Pillai MR, Chaturvedi V, Vignali DA. Regulatory T cell suppression is potentiated by target T cells in a cell contact, IL-35- and IL-10-dependent manner. J Immunol. 2009; 182:6121–6128. [PubMed: 19414764]
18. Rubtsov YP, Rasmussen JP, Chi EY, Fontenot J, Castelli L, Ye X, Treuting P, Siewe L, Roers A, Henderson WR Jr, Muller W, Rudensky AY. Regulatory T cell-derived interleukin-10 limits inflammation at environmental interfaces. Immunity. 2008; 28:546–558. [PubMed: 18387831]

19. Fontenot JD, Gavin MA, Rudensky AY. Foxp3 programs the development and function of CD4+CD25+ regulatory T cells. Nat Immunol. 2003; 4:330–336. [PubMed: 12612578]
20. Brunkow ME, Jeffery EW, Hjerrild KA, Paeper B, Clark LB, Yasayko SA, Wilkinson JE, Galas D, Ziegler SF, Ramsdell F. Disruption of a new forkhead/winged-helix protein, scurfin, results in the fatal lymphoproliferative disorder of the scurfy mouse. Nat Genet. 2001; 27:68–73. [PubMed: 11138001]
21. Tulone C, Tsang J, Prokopowicz Z, Grosvenor N, Chain B. Natural cathepsin E deficiency in the immune system of C57BL/6J mice. Immunogenetics. 2007; 59:927–935. [PubMed: 18000662]
22. Collison LW, Vignali DA. In vitro Treg suppression assays. Methods Mol Biol. 2011; 707:21–37. [PubMed: 21287326]
23. Workman CJ, Collison LW, Bettini M, Pillai MR, Rehg JE, Vignali DA. In vivo Treg suppression assays. Methods Mol Biol. 2011; 707:119–156. [PubMed: 21287333]
24. Rocke DM, Durbin B. Approximate variance-stabilizing transformations for gene-expression microarray data. Bioinformatics. 2003; 19:966–972. [PubMed: 12761059]
25. DiPaolo RJ, Brinster C, Davidson TS, Andersson J, Glass D, Shevach EM. Autoantigen-specific TGFbeta-induced Foxp3+ regulatory T cells prevent autoimmunity by inhibiting dendritic cells from activating autoreactive T cells. J Immunol. 2007; 179:4685–4693. [PubMed: 17878367]
26. Huter EN, Punkosdy GA, Glass DD, Cheng LI, Ward JM, Shevach EM. TGFbeta-induced Foxp3+ regulatory T cells rescue scurfy mice. Eur J Immunol. 2008; 38:1814–1821. [PubMed: 18546144]
27. Rocha B, Dautigny N, Pereira P. Peripheral T lymphocytes: expansion potential and homeostatic regulation of pool sizes and CD4/CD8 ratios in vivo. Eur J Immunol. 1989; 19:905–911. [PubMed: 2500349]
28. Workman CJ, Vignali DA. Negative regulation of T cell homeostasis by lymphocyte activation gene-3 (CD223). J Immunol. 2005; 174:688–695. [PubMed: 15634887]
29. Bell EB, Sparshott SM, Drayson MT, Ford WL. The stable and permanent expansion of functional T lymphocytes in athymic nude rats after a single injection of mature T cells. J Immunol. 1987; 139:1379–1384. [PubMed: 3305705]
30. Asseman C, Mauze S, Leach MW, Coffman RL, Powrie F. An essential role for interleukin 10 in the function of regulatory T cells that inhibit intestinal inflammation. J Exp Med. 1999; 190:995–1004. [PubMed: 10510089]
31. Izcue A, Coombes JL, Powrie F. Regulatory T cells suppress systemic and mucosal immune activation to control intestinal inflammation. Immunol Rev. 2006; 212:256–271. [PubMed: 16903919]
32. Gorelik L, Flavell RA. Abrogation of TGFbeta signaling in T cells leads to spontaneous T cell differentiation and autoimmune disease. Immunity. 2000; 12:171–181. [PubMed: 10714683]
33. Robinson MS, Bonifacino JS. Adaptor-related proteins. Curr Opin Cell Biol. 2001; 13:444–453. [PubMed: 11454451]
34. Zaidi N, Kalbacher H. Cathepsin E: a mini review. Biochem Biophys Res Commun. 2008; 367:517–522. [PubMed: 18178150]
35. Yasukochi A, Kawakubo T, Nakamura S, Yamamoto K. Cathepsin E enhances anticancer activity of doxorubicin on human prostate cancer cells showing resistance to TRAIL-mediated apoptosis. Biol Chem. 2010; 391:947–958. [PubMed: 20482316]
36. Kawakubo T, Okamoto K, Iwata J, Shin M, Okamoto Y, Yasukochi A, Nakayama KI, Kadowaki T, Tsukuba T, Yamamoto K. Cathepsin E prevents tumor growth and metastasis by catalyzing the proteolytic release of soluble TRAIL from tumor cell surface. Cancer Res. 2007; 67:10869–10878. [PubMed: 18006832]
37. Wang S, El-Deiry WS. TRAIL and apoptosis induction by TNF-family death receptors. Oncogene. 2003; 22:8628–8633. [PubMed: 14634624]
38. Hoffmann O, Zipp F, Weber JR. Tumour necrosis factor-related apoptosis-inducing ligand (TRAIL) in central nervous system inflammation. J Mol Med. 2009; 87:753–763. [PubMed: 19449143]
39. Kimberley FC, Screaton GR. Following a TRAIL: update on a ligand and its five receptors. Cell Res. 2004; 14:359–372. [PubMed: 15538968]

40. Ren X, Ye F, Jiang Z, Chu Y, Xiong S, Wang Y. Involvement of cellular death in TRAIL/DR5-dependent suppression induced by CD4(+)CD25(+) regulatory T cells. Cell Death Differ. 2007; 14:2076–2084. [PubMed: 17762882]
41. Griffith TS, Brincks EL, Gurung P, Kucaba TA, Ferguson TA. Systemic immunological tolerance to ocular antigens is mediated by TRAIL-expressing CD8+ T cells. J Immunol. 2010; 186:791–798. [PubMed: 21169546]
42. Gregoli PA, Bondurant MC. Function of caspases in regulating apoptosis caused by erythropoietin deprivation in erythroid progenitors. J Cell Physiol. 1999; 178:133–143. [PubMed: 10048577]
43. Bossen C, Ingold K, Tardivel A, Bodmer JL, Gaide O, Hertig S, Ambrose C, Tschopp J, Schneider P. Interactions of tumor necrosis factor (TNF) and TNF receptor family members in the mouse and human. J Biol Chem. 2006; 281:13964–13971. [PubMed: 16547002]
44. Kayagaki N, Yamaguchi N, Nakayama M, Eto H, Okumura K, Yagita H. Type I interferons (IFNs) regulate tumor necrosis factor-related apoptosis-inducing ligand (TRAIL) expression on human T cells: A novel mechanism for the antitumor effects of type I IFNs. J Exp Med. 1999; 189:1451–1460. [PubMed: 10224285]
45. Zhang XR, Zhang LY, Devadas S, Li L, Keegan AD, Shi YF. Reciprocal expression of TRAIL and CD95L in Th1 and Th2 cells: role of apoptosis in T helper subset differentiation. Cell Death Differ. 2003; 10:203–210. [PubMed: 12700648]
46. Wohlfert E, Belkaid Y. Plasticity of T reg at infected sites. Mucosal Immunol. 2010; 3:213–215. [PubMed: 20237465]
47. Backus GS, Howden R, Fostel J, Bauer AK, Cho HY, Marzec J, Peden DB, Kleeberger SR. Protective role of interleukin-10 in ozone-induced pulmonary inflammation. Environ Health Perspect. 2010; 118:1721–1727. [PubMed: 20826374]
48. Monleon I, Martinez-Lorenzo MJ, Monteagudo L, Lasierra P, Taules M, Iturralde M, Pineiro A, Larrad L, Alava MA, Naval J, Anel A. Differential secretion of Fas ligand- or APO2 ligand/TNF-related apoptosis-inducing ligand-carrying microvesicles during activation-induced death of human T cells. J Immunol. 2001; 167:6736–6744. [PubMed: 11739488]
49. Mariani SM, Krammer PH. Differential regulation of TRAIL and CD95 ligand in transformed cells of the T and B lymphocyte lineage. Eur J Immunol. 1998; 28:973–982. [PubMed: 9541592]
50. Gorham JD, Guler ML, Steen RG, Mackey AJ, Daly MJ, Frederick K, Dietrich WF, Murphy KM. Genetic mapping of a murine locus controlling development of T helper 1/T helper 2 type responses. Proc Natl Acad Sci U S A. 1996; 93:12467–12472. [PubMed: 8901605]
51. Okamoto M, Van Stry M, Chung L, Koyanagi M, Sun X, Suzuki Y, Ohara O, Kitamura H, Hijikata A, Kubo M, Bix M. Mina, an Il4 repressor, controls T helper type 2 bias. Nat Immunol. 2009; 10:872–879. [PubMed: 19561615]

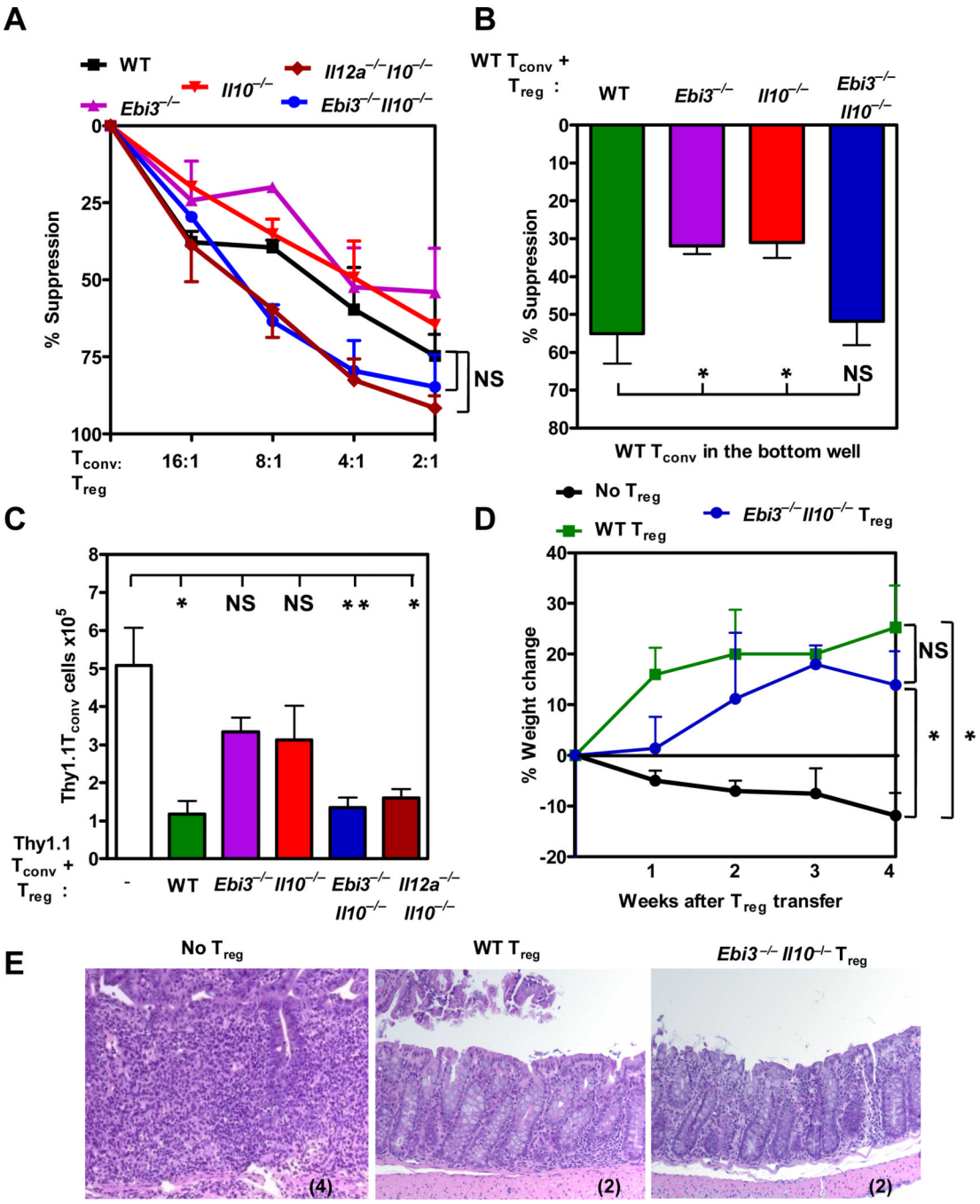

Figure 1. ***Ebi3*$^{-/-}$*Il10*$^{-/-}$ T$_{regs}$ are suppressive *in vitro* and *in vivo***

(A) Wild type or knock out T$_{reg}$ purified by FACS were titrated in a standard T$_{reg}$ assay with T$_{conv}$ cells and anti-CD3 and anti-CD28 coated latex beads. Proliferation of T$_{conv}$ responder cells was determined by [^{3}H]-thymidine incorporation (p-value: wild type T$_{regs}$ compared to *Ebi3*$^{-/-}$*Il10*$^{-/-}$, and *Il12a*$^{-/-}$*Il10*$^{-/-}$ T$_{regs}$, Not significant (NS)). (B) Wild type or knock out T$_{reg}$ were cultured with anti-CD3 and anti-CD28 coated latex beads and T$_{conv}$ cells in the inserts of a Transwell™ culture plate. Third party, wild type responder T$_{conv}$ was activated in the bottom chamber of the plate. Proliferation of responder cells was determined by [^{3}H]-thymidine incorporation. Proliferation ranged from 30,000–60,000 cpm. p-value: *: <0.05, NS: Not significant. (C) Congenically marked wild type T$_{conv}$ cells, wild type or knock out

T_{regs} purified by FACS were injected at 4:1 ratio into *Rag1*$^{-/-}$ mice. $CD4^+$ cell numbers in the spleen were analyzed after 7 days by flow cytometry. p-value: * <0.05. (D) Wild type T_{conv} cells (0.5×10^6) were injected into *Rag1*$^{-/-}$ mice. The weight of the mice was monitored weekly for weight loss. Once the mice had lost 5% of its body weight wild type or knock out T_{regs} were injected. Mice were monitored for percent weight change calculated based on the weight at the time of T_{reg} injection. p-value: * <0.05 and NS: Not significant. (E) Colonic tissue sections stained with H & E stain were scored in a blinded manner. Representative images of sections from 3 independent experiments are shown with histological score in parentheses. Data represent the mean ± SEM of (A) 3, (B) 3–5, (C) 4–9 mice per group, (D&E) 3 independent experiments.

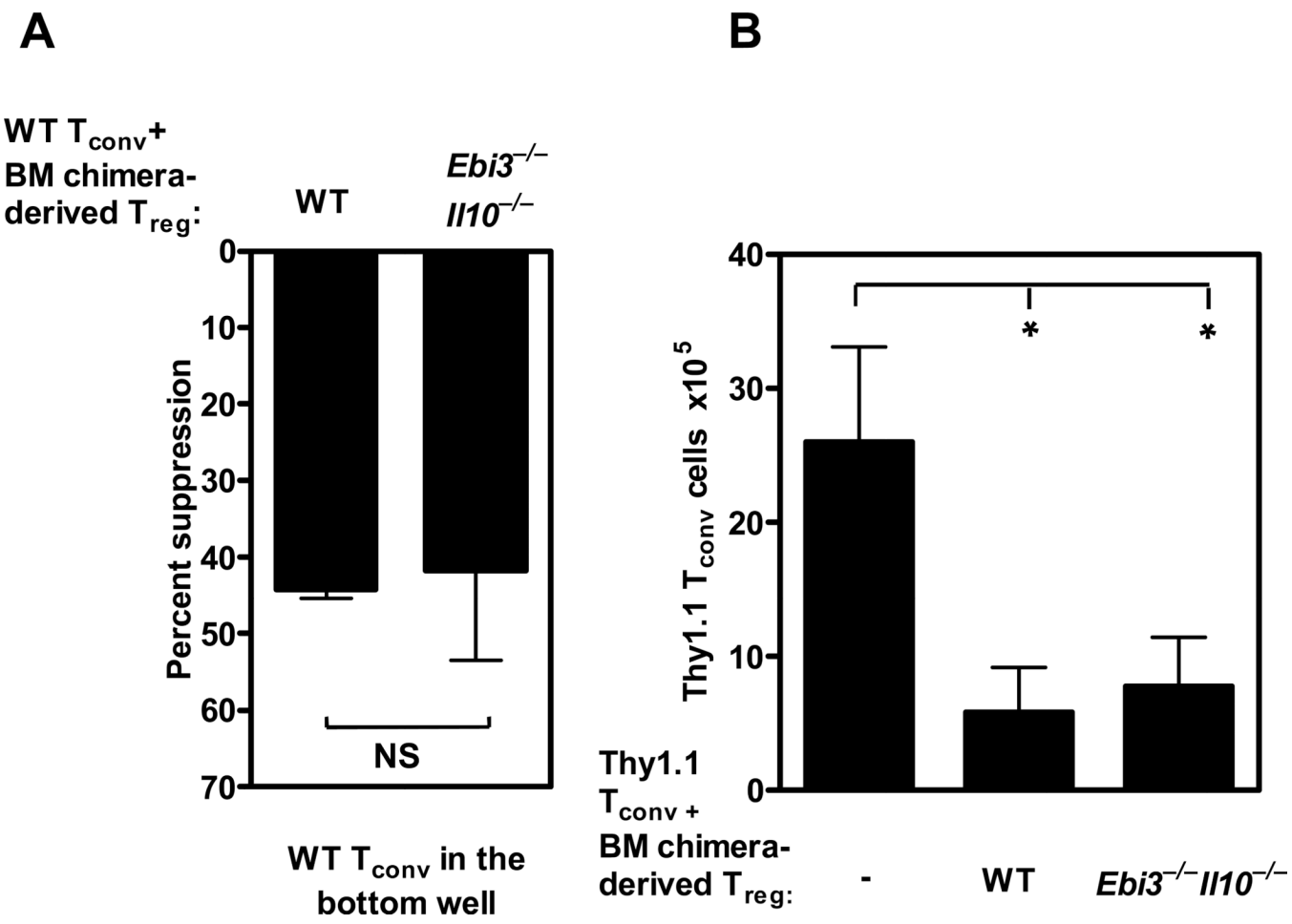

Figure 2. ***Ebi3*$^{-/-}$*Il10*$^{-/-}$ T_{regs} that developed in a mixed bone marrow chimera can function *in vitro* and *in vivo***

Congenically labeled wild type bone marrow and knock out bone marrow was mixed at a 1:1 ratio and injected into sub lethally irradiated *Rag1*$^{-/-}$ mice. (A) After 8 weeks Thy.1.2^{+} wild type T_{reg} cells or knock out T_{reg} cells were purified by FACS from the bone marrow chimeric mice and cultured in the inserts of a Transwell™ plate in the presence of wild type T_{conv} cells and anti-CD3 and anti-CD28 coated latex beads. Wild type naive T_{conv} cells were activated in the presence of anti-CD3 and anti-CD28 coated beads in the bottom chamber of a Transwell™ for 72 h. Proliferation was determined by [^{3}H]-thymidine incorporation. Data represents the mean± SEM of two independent experiments. (p-value; NS: Not significant). (B) Purified wild type or *Ebi3*$^{-/-}$*Il10*$^{-/-}$ bone marrow chimera-derived T_{regs} were injected into *Rag1*$^{-/-}$ mice in the presence of congenically marked naïve T_{conv} cells. The expansion of naïve Thy1.1 CD4^{+} T cells were assessed by flow cytometry. Data represents the mean ± SEM of two independent experiments with 3–4 mice per group (p-value *=0.06).

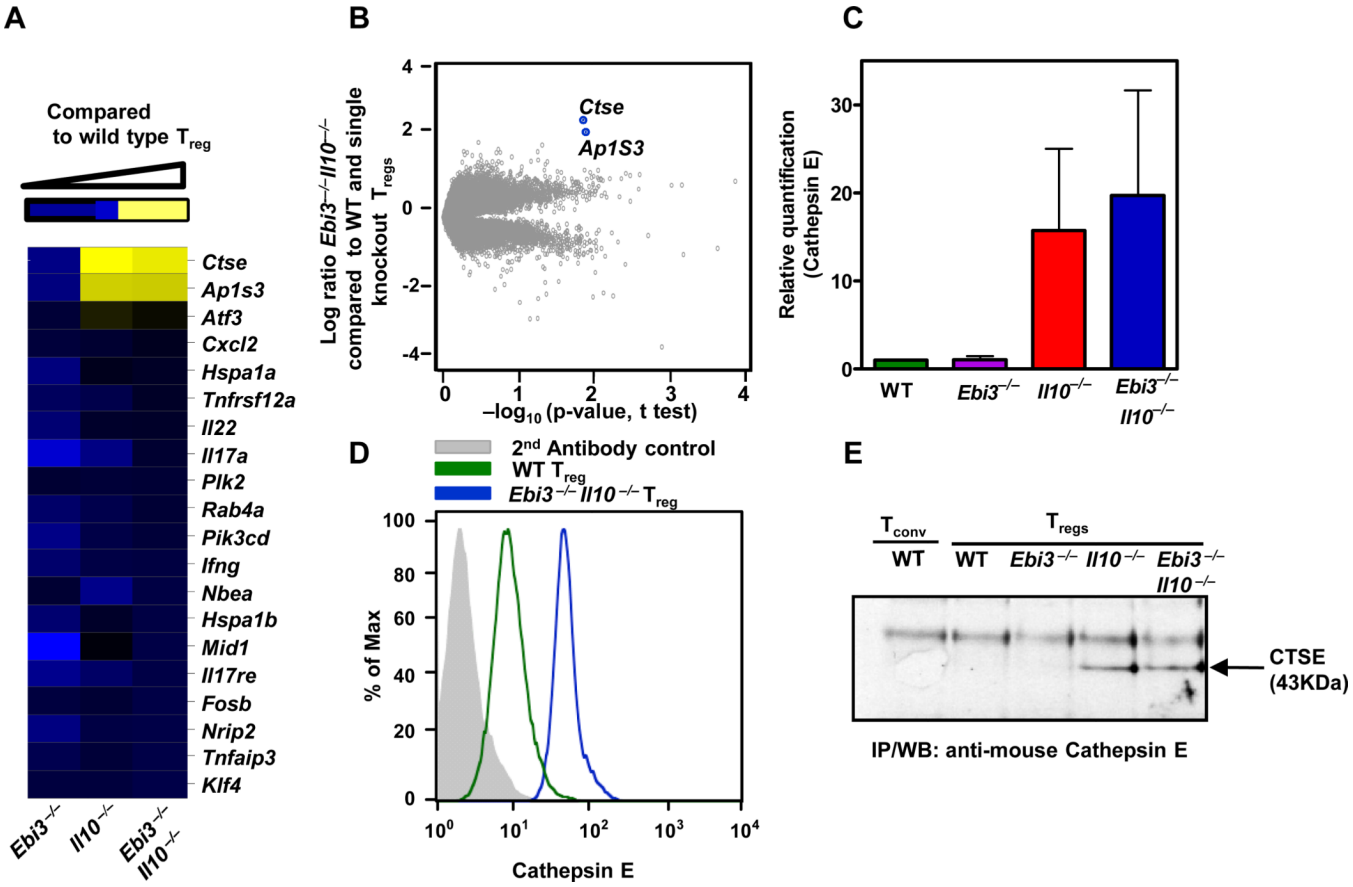

Figure 3. Up-regulation of CTSE by *Ebi3*$^{-/-}$*Il10*$^{-/-}$ T$_{regs}$

(A) mRNA was isolated from wild type or knock out T$_{reg}$ purified by FACS and used for Affymetrix analysis. Modulated genes in knock out T$_{reg}$ compared to wild type T$_{regs}$ is depicted in a heat map. (B) Volcano plot comparing wild type and *Ebi3*$^{-/-}$ *Il10*$^{-/-}$, T$_{regs}$. Highest modulated genes are marked. (C) mRNA was isolated from wild type or knock out T$_{reg}$ purified by FACS, cDNA synthesized and *Ctse* expression assessed by qPCR. Data are the mean of 2 independent experiments. (D) Wild type or knock out T$_{reg}$ were stained for intracellular CTSE [grey - 2nd antibody control, open histograms; in green - wild type T$_{regs}$ and in blue; *Ebi3*$^{-/-}$ *Il10*$^{-/-}$ T$_{regs}$]. (E) Equal numbers of FACS purified wild type or knock out T$_{reg}$ were lysed, CTSE immunoprecipitated and analysed by SDS-PAGE/western blot. Data are representative (A, B, D and E) of three independent experiments.

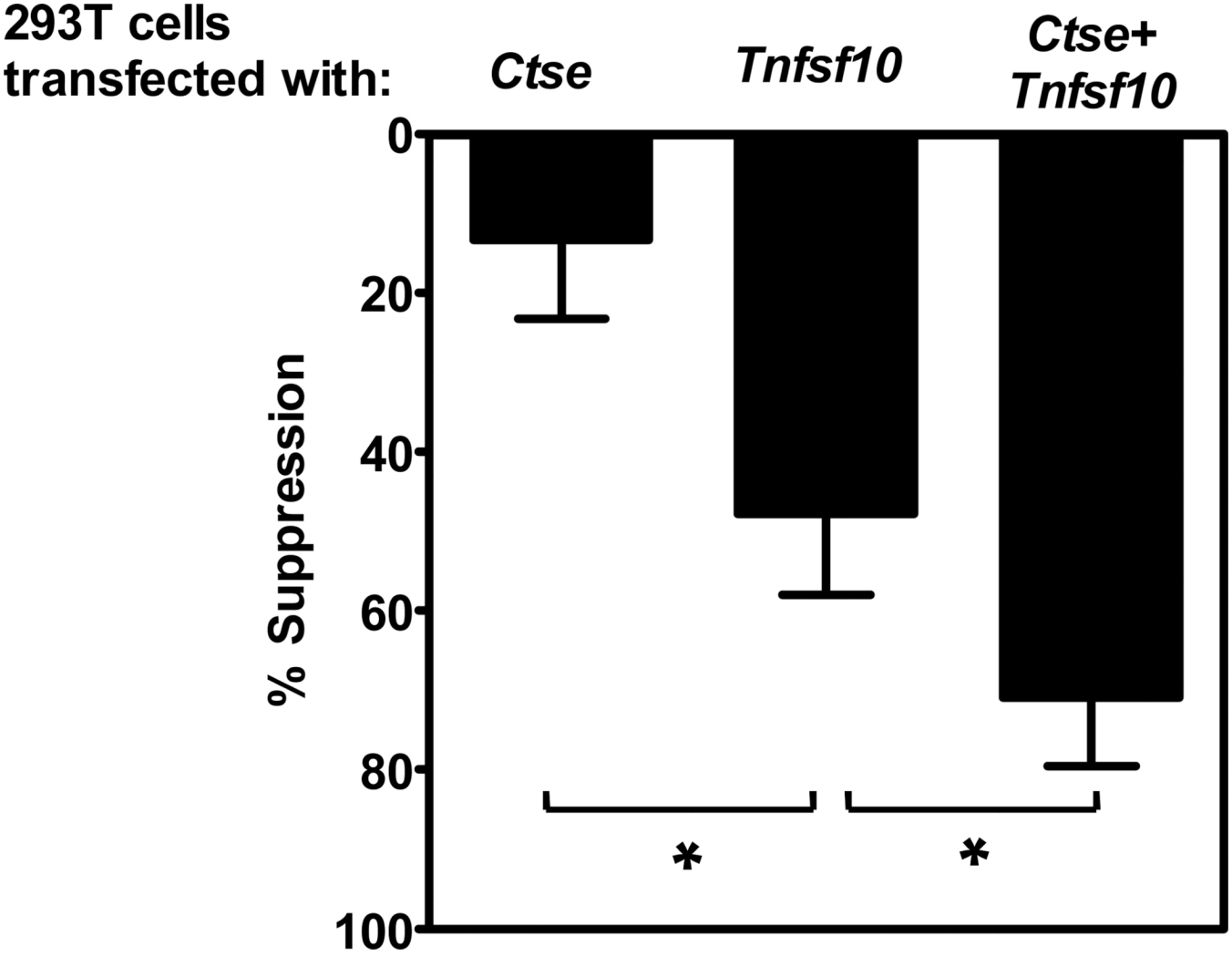

Figure 4. Cathepsin E enhances the suppression of T_{conv} cells by TRAIL

293T cells were transfected either with *Ctse* and *Tnfsf10* alone or together. The cells were irradiated with 3000 rads 48h post transfection and seeded at a density of 7000 cells per well in a 96 well flat bottom plate. Freshly isolated C57BL/6 T_{conv} cells were added to the seeded plate at 8×10^4 per well and stimulated with anti-CD3 and anti-CD28 coated beads for 72 hours. Proliferation of responder cells was determined by [^{3}H]-thymidine incorporation. T_{conv} cell proliferation was calculated by subtracting the basal [3H]-thymidine incorporation of irradiated 293T plus T cells without anti-CD3 and anti-CD28 stimulation. Data represent the average of three independent experiments. p-value, * : <0.05.

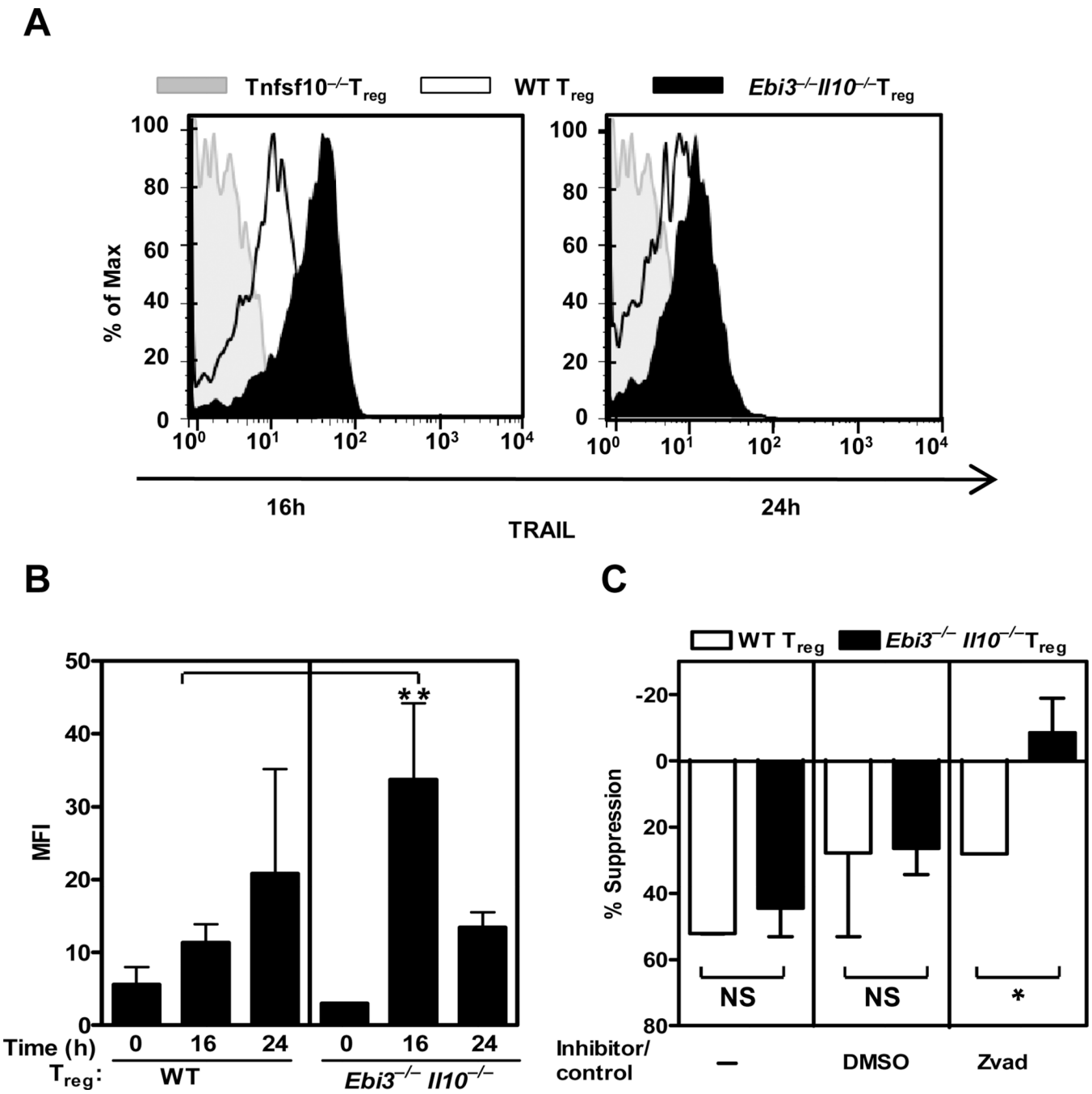

Figure 5. TRAIL dependence and modulation in *Ebi3*$^{-/-}$ *Il10*$^{-/-}$T$_{regs}$

Wild type or knock out T$_{reg}$ purified by FACS were activated in presence of anti-CD3 and anti-CD28 coated latex beads with IL2 for 16 and 24h. (A) Cells were collected and surface TRAIL expression detected by flow cytometry using an anti-mouse TRAIL antibody. Data are representative of 3 independent experiments. (B) Mean fluorescence intensity (MFI) of surface TRAIL expression following activation from 3–4 independent experiments were plotted. Students t Test; p-value ** = <0.05. (C) Wild type or knock out T$_{reg}$ were cultured in the insert of a Transwell™ culture plate in the presence of wild type T$_{conv}$ cells. zVAD or DMSO control was added to the Transwell™ assay. Freshly purified wild type responder T$_{conv}$ cells were activated in the bottom chamber of the plate. Proliferation of responder

cells was determined by [^{3}H]-thymidine incorporation. Data represent the mean ± SEM of 2 independent experiments. p-value * = 0.07.

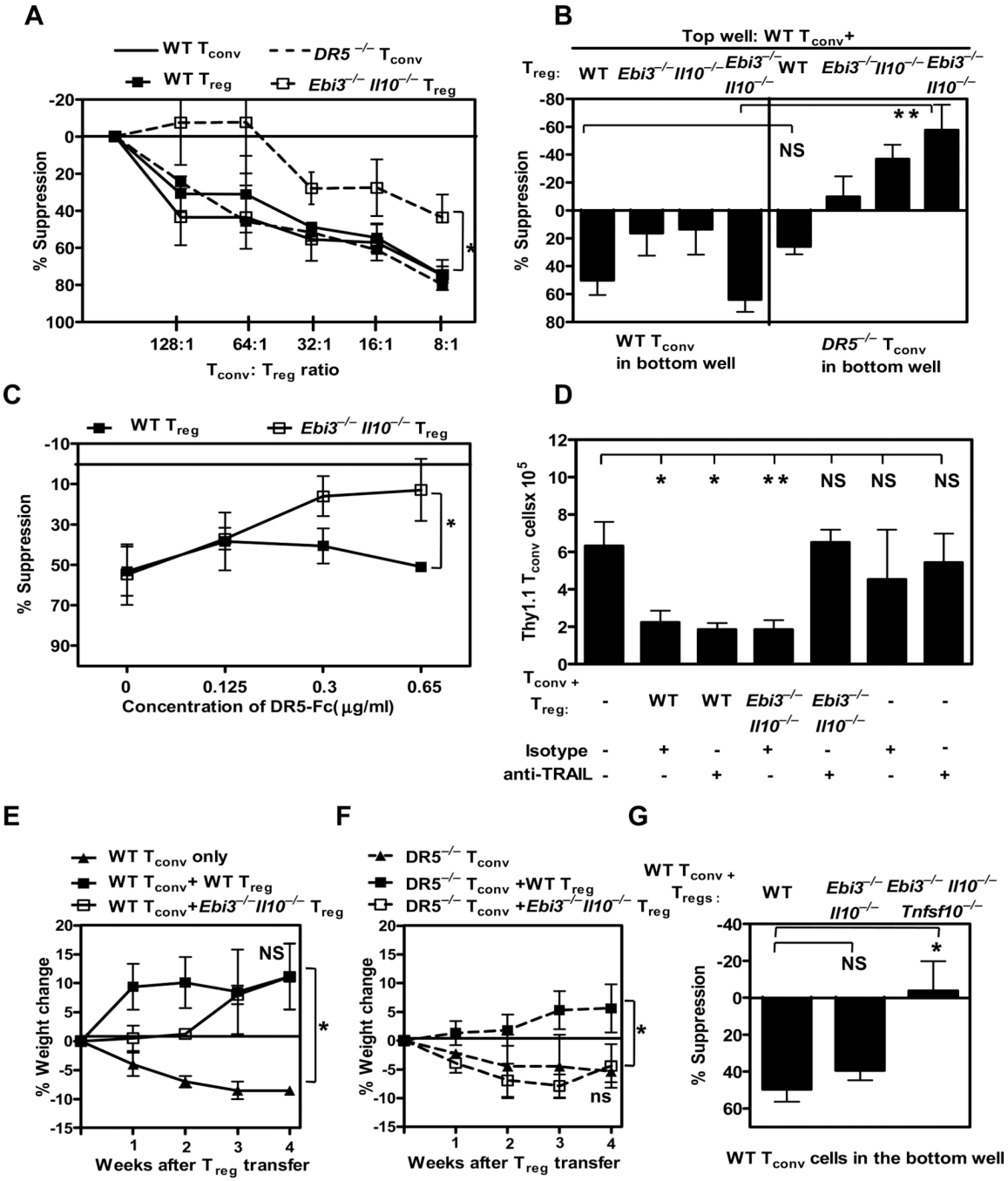

Figure 6. *Ebi3*$^{-/-}$*Il10*$^{-/-}$ T_{reg} mediated suppression is TRAIL-dependent

Wild type or knock out T_{regs} purified by FACS (A) were titrated in a T_{reg} assay with wild type or DR5$^{-/-}$ T_{conv} cells and stimulated with anti-CD3 and anti-CD28 coated latex beads or (B) were cultured with wild type T_{conv} cells in the insert of a Transwell™ culture plate. Wild type or DR5$^{-/-}$ T_{conv} cells were activated in the bottom chamber of the plate with anti-CD3 and anti-CD28 coated latex beads. Proliferation of responder wild type or DR5$^{-/-}$ T_{conv} cells was determined by [^{3}H]-thymidine incorporation. CPM ranged between 30,000–65,000. Results shown here are average of 4–5 independent experiments. (C) Wild type and *Ebi3*$^{-/-}$*Il10*$^{-/-}$ T_{regs} were stimulated with anti-CD3 and anti-CD28 coated latex beads in the presence of T_{conv} cells in the insert of a Transwell™ culture plate. Freshly purified wild type

responder T_{conv} cells were activated in the bottom wells in the presence of a titrated amount of DR5-Fc. Data is average of 2–3 independent experiments, One way ANCOVA p-value *= 0.01 (D) Congenically marked wild type T_{conv} cells and wild type or knock out T_{regs} were injected at 4:1 ratio in to *Rag*$^{-/-}$ mice. On days 1 and 3 TRAIL neutralizing mAb or isotype control were injected by i.p. CD4, Thy1.1 and Thy 1.2 T cell numbers in the spleen were analyzed after 7 days by flow cytometry. Data includes 3–6 mice per group from 3 independent experiments. (E) Wild type littermate control T_{conv} cells or (F) DR5$^{-/-}$ T_{conv} cells (0.5×10^6 cells) were injected into *Rag1*$^{-/-}$ mice. The weight of the mice was monitored weekly for weight loss. Percent weight change was calculated based on the weight at the time of T_{reg} injection. (G) Wild type or knock out T_{regs} purified by FACS were cultured with wild type T_{conv} cells in the insert of a Transwell™ culture plate. Wild type T_{conv} cells were activated in the bottom chamber of the plate with anti-CD3 and anti-CD28-coated latex beads. Proliferation of responder T_{conv} cells was determined by [^{3}H]-thymidine incorporation. CPM ranged between 30,000–70,000. Results shown here are mean ± SEM of 3 independent experiments. p-value - A–G; *: < 0.05, ** < 0.005, NS: Not significant.

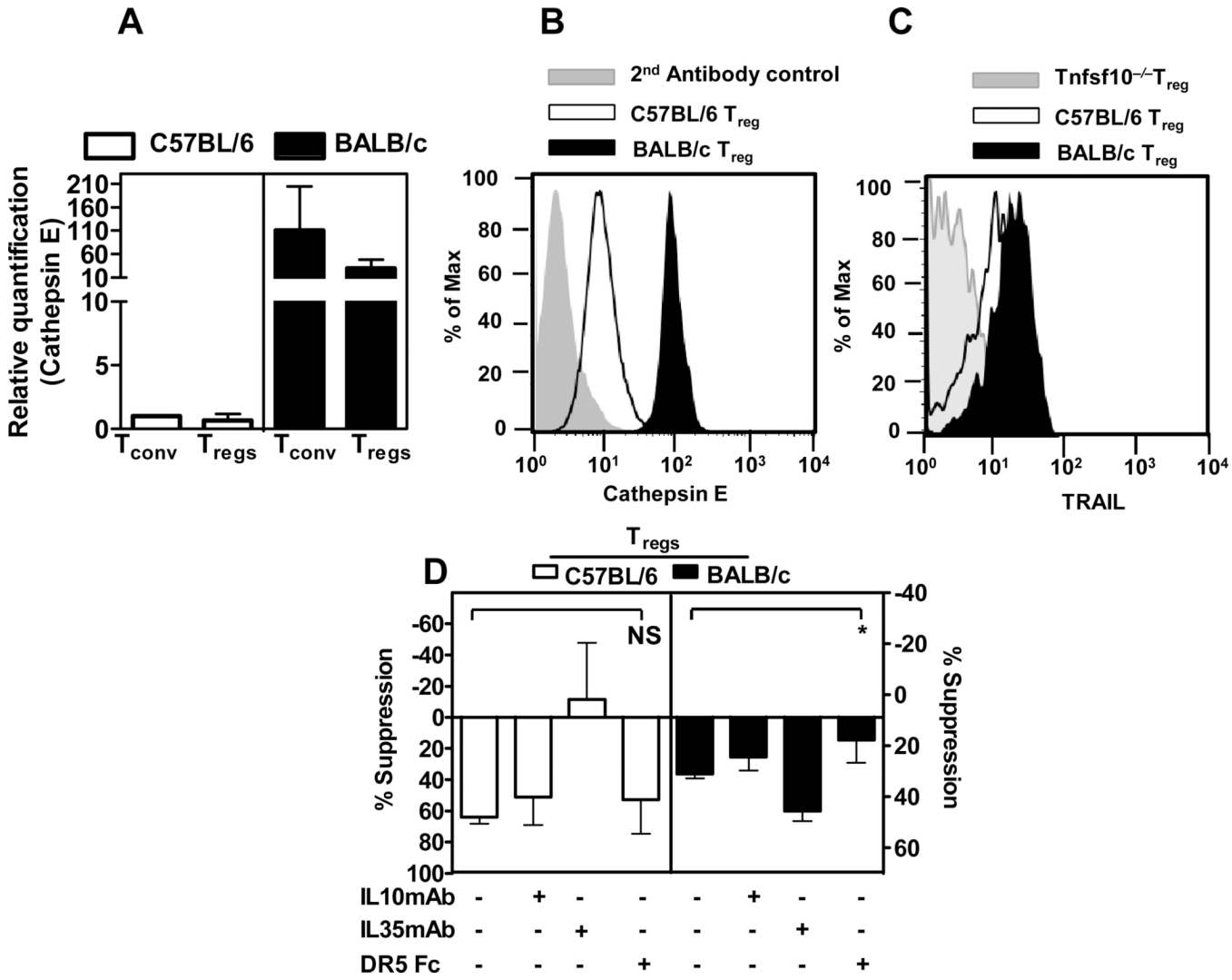

Figure 7. BALB/c T_{reg} preferentially use TRAIL-mediated pathways compared to C57BL/6 T_{regs}

(A) mRNA was isolated from freshly purified C57BL/6 or BALB/c T_{conv} cells and T_{regs}, cDNA synthesized and qPCR performed to assess *Ctse* expression. (B) Intracellular staining for CTSE was performed with purified C57BL/6 or BALB/c T_{reg} [Grey filled - secondary antibody only control; open histogram - C57BL/6 T_{regs} and closed histogram BALB/c T_{regs}]. (C) TRAIL staining was performed with *Tnfsf10*$^{-/-}$, wild type C57BL/6 or BALB/c T_{regs}, activated in presence of anti-CD3 and anti-CD28 coated latex beads with IL2 for 16h and surface TRAIL expression was detected by flow cytometry using a anti-mouse TRAIL antibody (MFI from three independent experiments, p-value:0.07). (D) Wild type C57BL/6 or BALB/c T_{regs} were mixed at 1:2 ratio with naïve wild type T_{conv} cells in the presence of anti-CD3 and anti-CD28 coated beads in the insert of a Transwell™ culture plate for 72h. Neutralizing antibodies against IL-10, IL-35 or a DR5-Fc protein were added to the Transwell™ assay at pre-determined concentrations as described in the methods. Freshly purified wild type responder T_{conv} were activated in the bottom chamber of a Transwell™ culture plate. Proliferation of the responder cells was determined by [^{3}H]-thymidine incorporation. p-value *: < 0.05. Data represent 3–4 independent experiments.